Temporal regulation of *ZBTB16* expression by glucocorticoids alters human cortical neurogenesis

Anthi C. Krontira[1,2], Cristiana Cruceanu[1,3], Christina Kyrousi[4,5,6], Leander Dony[1,2,7,8], Marie-Helen Link[1], Nils Kappelmann[1,2], Dorothee Pöhlchen[1,2], Simone Roeh[1], Vincenza Sportelli[1], Barbara Wölfel[1], Maik Ködel[1], Susann Sauer[1], Monika-Rex-Haffner[1], Marta Labeur[1], Silvia Cappello[4], Elisabeth B. Binder[1]

1. Department of Translational Research in Psychiatry, Max Planck Institute of Psychiatry, Munich, Germany, 80804 Munich, Germany
2. International Max Planck Research School for Translational Psychiatry, Munich, Germany, 80804 Munich, Germany
3. Department of Physiology and Pharmacology, Karolinska Institutet, Stockholm Sweden
4. Developmental Neurobiology, Max Planck Institute of Psychiatry, 80804 Munich, Germany
5. First Department of Psychiatry, Medical School, National and Kapodistrian University of Athens, Eginition Hospital, Greece
6. University Mental Health, Neurosciences and Precision Medicine Research Institute "Costas Stefanis", Athens, Greece
7. Department for Computational Health, Helmholtz Munich, 85764 Neuherberg, Germany
8. TUM School of Life Sciences Weihenstephan, Technical University of Munich, 85354 Freising, Germany

Corresponding author

Elisabeth B. Binder: binder@psych.mpg.de

Summary

Glucocorticoids are important for proper organ maturation[1]. Increased exposure to these hormones during pregnancy, as a result of commonly prescribed synthetic glucocorticoids such as dexamethasone in preterm births[2], has been associated with lasting effects on the offspring, including on neurodevelopment and neuropsychiatric disease risk[3]. While the consequences of glucocorticoid excess in term and especially adult brain have been extensively studied, mainly in rodents[4], studies on their effects during early human cortical development are absent. Here we use human cerebral organoids and mice to study cell-type specific effects of glucocorticoids on neurogenic processes. We show that glucocorticoid administration during neurogenesis alters the cellular architecture of the developing cortex by increasing a specific type of gyrencephalic species-enriched basal progenitors that co-express *PAX6* and *EOMES*. This effect is mediated via the glucocorticoid-responsive transcription factor *ZBTB16* as shown with overexpression, genetic knock-down and reporter assays experiments in organoids and embryonic mouse models and leads to increased production of deep-layer neurons. A phenome-wide mendelian randomization analysis of a genetic intronic enhancer variant that moderates glucocorticoid-induced *ZBTB16* levels, as shown with enhancer assays and enhancer-editing in organoids, reveals potential causal relationships with increased educational attainment as well as neuroimaging phenotypes in adults. In this study we provide a cellular and molecular pathway for the effects of glucocorticoids on human neurogenesis that potentially explains postnatal phenotypes and may be used to refine treatment guidelines.

Main

Prenatal development relates to postnatal health. The 'developmental origin of health and disease (DOHaD) hypothesis'[5] proposes that environmental exposures during critical prenatal periods have lasting effects on cells

44 and tissues impacting human health throughout life. This is also true for the central nervous system (CNS) with a
45 number of environmental factors shown to impact its cellular architecture and function[6].
46 An important factor shown to affect CNS development during pregnancy are glucocorticoids (GCs)[7]. These steroid
47 hormones are endogenously present prenatally with a physiological rise close to term, important for the maturation
48 of fetal organs[1]. Exposure to levels of prenatal GCs outside of the physiological range has been related to lasting
49 postnatal effects[3]. An important exposure that results in GC excess is the therapeutic use of synthetic GCs (sGCs)
50 during pregnancy. While the placenta constitutes a protective barrier for endogenous maternal GCs, i.e. cortisol
51 with only as little as 10% of the circulating hormones reaching the fetal compartments, sGCs readily cross the
52 placenta[8] leading to higher exposure of the fetus. sGCs, either betamethasone or dexamethasone, are most
53 commonly prescribed starting at 24 and until 33 gestational weeks (GWs) in pregnancies with high risk for preterm
54 delivery, to facilitate fetal lung maturation[2]. More than 1 in 10 babies are born prematurely every year, a number
55 which amounts to ~15 million preterm births (< 37 GWs) per year[9] of which ~ 615,000 are born extremely preterm
56 (< 28 GWs)[10], highlighting the clinical and societal importance of prenatal sGCs use. Dexamethasone is also
57 administered throughout pregnancy, starting as early as GW6, to female fetuses at risk of virilization due to
58 congenital adrenal hyperplasia[8]. Given the clear beneficial anti-inflammatory effects of sGCs, they are also used
59 during the COVID-19 pandemic in patients requiring oxygen therapy and mechanical ventilation[11]. Pregnant women
60 were not excluded from this treatment course, with the guidelines specifically promoting the use of dexamethasone
61 in women that fulfill the afore-mentioned criteria[12].
62 The overall molecular and cellular effects of GCs on the term and adult brain are well-characterized in rodents[4].
63 Interestingly, their effects on early stages of brain development and especially during the neurogenic period, which
64 extends till GW28[13] in humans and thus in the timeframe of sGCs administration for extremely preterm births, have
65 rarely been studied and are absent for human brain or complex models of the human developing cortex. To gain a
66 better molecular and cellular understanding of GC effects on neurogenic processes of the developing human
67 neocortex, we used human cerebral organoids (hCOs) to investigate GC impact on neurogenesis and on the
68 molecular and transcriptional landscape as well as potential mediation of postnatal phenotypes and validated
69 important phenotypes using *in vivo* mouse models.
70
71 **Glucocorticoids increase the number of basal progenitors**
72 To study GC effects on neurogenic trajectories in the developing neocortex we treated hCOs[14] for 7 days with
73 100nM of dexamethasone (dex), a dose and time consistent with therapeutic guidelines followed in clinical settings[2]
74 (see Methods for detailed explanation). This treatment was initiated at day 43 (Fig.1a) in hCOS derived from 2
75 independent iPSC (induced pluripotent stem cell) lines. Days 40-50 were chosen as a time-range when hCOs are
76 actively performing neurogenic processes with all the progenitor cell types present while birth of deep layer neurons
77 is peaking and of upper layer neurons has started[15]. First, we analyzed the specific effects of dex on different
78 progenitor cell types defined by the expression of PAX6 (Paired Box 6) and EOMES (Eomesodermin - also known
79 as T-box brain protein 2 or TBR2). PAX6 is highly expressed in radial glia (RG) cells, EOMES, but not PAX6, in
80 intermediate basal progenitors (IPs), while both can be expressed in certain basal progenitors (BPs). Dex
81 consistently led to a significant increase of PAX6+EOMES+ BPs (Fig.1b,c) in hCOs derived from both iPSC lines
82 compared to veh-treated hCOs. The increased PAX6+EOMES+ BPs were localized in the basal side of the germinal
83 zones, in the subventricular-like zone (SVZ) (Fig.1d and Extended data Fig.1). Moreover, we confirmed the effects
84 of dex on the increase of double-positive BPs by analyzing the number of PAX6+EOMES-, PAX6-EOMES+ and
85 PAX6+EOMES+ progenitor subtypes in Line 2- hCOs using flow cytometry analysis (FCa). We observed a
86 significant increase (+18%) in PAX6+EOMES+ BPs when hCOs were treated with dex compared to veh (Extended

data Fig. 2a-c). Co-administration of the glucocorticoid receptor (GR) antagonist RU486 supported that dex effects are mainly mediated by the GR and not the mineralocorticoid receptor (Extended data Fig. 2a,d,e).

Focusing on neurons, dex led to an increase of immature neuronal somata (doublecortin, DCX+) in the ventricular-like-zone (VZ, Fig.1e,f) and to a decrease of the DCX zone thickness in the cortical-like plate (CP, Fig.1e,g), potentially pointing to later-born neurons still migrating to their final destination. This putatively prolongated neurogenesis can be related to the increased numbers of PAX6+EOMES+ BPs. These BPs have high proliferative capacity, undergoing not only neurogenic but also self-renewing proliferative divisions, which comes in contrast to PAX6-EOMES+ IPs that primarily undergo one neurogenic division producing two neurons[16–21]. Interestingly, PAX6+EOMES+ BPs are abundant in the inner and outer SVZ of mammals with a gyrified brain, such as ferrets, primates and humans, and are one of the mechanisms responsible for the increased neurogenic potential of these species[17]. In lissencephalic species, like rodents, this cell type is rare with the vast majority of BPs being IPs[16–21]. Overall, GCs seem to increase neurogenic processes that are enriched in gyrified species, highlighting how an environmental factor can affect neurogenesis and subsequently the cellular architecture of the brain.

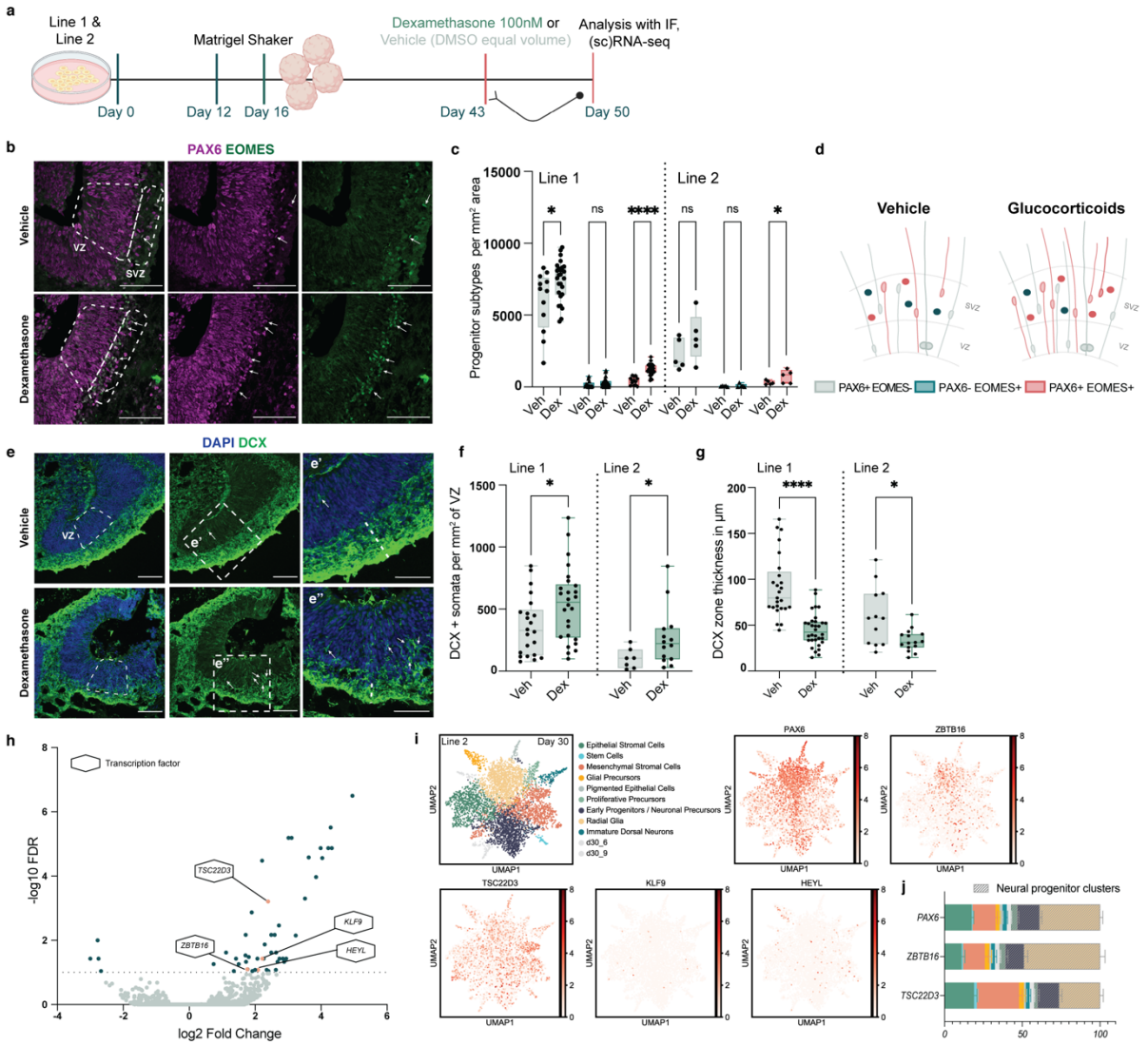

Figure 1l Glucocorticoids increase basal progenitors that co-express PAX6 and EOMES. a, Treatment and analysis workflow in human cerebral organoids (hCOs) derived from two iPSC lines. **b,** Representative images of day 50 hCOs at veh and dex conditions stained for PAX6 and EOMES. Arrows indicate cells that co-express PAX6 and EOMES; Scale bars, 100µm. **c,** Quantification of the progenitor subtypes in each treatment condition normalized by mm² of quantified total area in hCOs produced from two iPSC lines. **d**, Schematic representation of the effects of dex on progenitors, highlighting the increased numbers of basal

progenitors co-expressing PAX6 and EOMES. **e,** Representative images of day 50 hCOs at vehicle and dex conditions stained for DCX and DAPI. Arrows indicate DCX positive somata in the VZ; Scale bars, 100µm. **e' and e'',** Zoom-ins of the areas shown in vehicle and dex ventricles respectively in figure e. **f,** Quantification of DCX somata found in the VZ normalized per mm^2 of area. **g,** Quantification of DCX zone thickness in µm. **h,** Volcano plot of DE gene expression analysis in bulk RNA sequencing. Grey dots, genes with non-significant expression changes at an FDR cutoff of 10%; Blue dots, genes with significant expression changes; Orange dots denote TFs labeled with their gene name. **i,** UMAP plots of cell clusters and TFs in day 30 Line-2 hCOs from Cruceanu et al., 2022. **j,** Percent of the fraction of total of cells positive for each TF in each cluster. Color scheme follows the one in Fig.1i. FDR, false discovery rate with Benjamini-Hochberg correction. DMSO, dimethyl sulfoxide; IF, Immunofluorescence; Seq, sequencing; Veh, vehicle; Dex, dexamethasone; VZ, ventricular-like zone; SVZ, subventricular-like zone; BPs, basal progenitors; TFs, transcription factors. Significance was tested with two tailed Mann-Whitney comparison between treatment and vehicle. P-values: **** <=0.0001, * <=0.05, ns >0.05

Transcriptional response to glucocorticoids during neurogenesis

We next aimed to identify genes and pathways responsible for the effects of GCs on neurogenesis. For this we used bulk RNA sequencing (RNA-seq) of Line 2- day 45 hCOs following the exact treatment paradigm as above (100nM of dex or vehicle for 7 days, treatment start at day 38). At a 10% FDR cutoff, fifty genes were differentially expressed (DE) (Extended data Table 1). Given the essential role and developmental specificity of transcription factors (TFs) in determining neurodevelopmental processes[22], we decided to focus on this class of proteins. Out of the 50 DE genes only 4 were TFs, *TSC22D3* (TSC22 Domain family member 3), *KLF9* (Kruppel-like factor 9), *ZBTB16* (Zinc finger and BTB domain-containing protein 16) and *HEYL* (HEY-like protein) (Fig.1h). To narrow in on progenitor-specific responses, we took advantage of a single-cell (sc)RNA-seq cerebral organoid dataset that we previously published[15] (Line 2, 30 days). From the four TFs, *KLF9* and *HEYL* were very lowly expressed in hCOs, thus excluded as candidates (Fig.1i). *TSC22D3* had a ubiquitous expression pattern with the minority of TSC22D3+ cells located in neural progenitor clusters (42.5% of TSC22D3+ cells located in "Proliferative Precursors", "Neural Precursors", "Radial Glia" clusters, Extended data Table 2). In contrast, *ZBTB16* was enriched in the neural progenitor clusters (64.7% of ZBTB16+ cells), following the expression pattern of *PAX6* (Fig.1i,j). *ZBTB16* (also known as *PLZF*- promyelocytic leukemia zinc finger protein) has been associated with the regulation of the balance between self-renewal and differentiation of stem cells in multiple organ systems including the brain[23], so we decided to focus on this TF. It belongs to the Krüppel-like zinc finger family of TFs and is very well conserved across species. It has nine zinc finger motifs in the C terminus that comprise the DNA binding domain of the protein, a protein-protein interaction domain at the N terminus and a less well characterized middle RD2 (repressor domain 2) domain and can act as a transcriptional activator or repressor[23].

Glucocorticoids alter the very dynamic neurodevelopmental expression pattern of *ZBTB16*

ZBTB16 is dynamically expressed during rodent and human neurodevelopment with high brain expression early in gestation and a subsequent downregulation to low levels. In rodents, *Zbtb16* is expressed until E10.5 (embryonic day 10.5) in the forebrain[24] when it is downregulated to non-detectable levels during neurogenesis (Extended data Fig. 3a,b). In contrast, in human fetal cortex *ZBTB16* is expressed during the initial stages of neurogenesis (Extended data Fig. 3c), indicating expression of this TF during the neurogenic period in humans but not in rodents. We analyzed the *ZBTB16* expression pattern in our model of the developing human neocortex, the hCOs. *ZBTB16* was dynamically expressed in hCOs with high RNA (Fig.2a) and protein (Fig.2b) levels at the early stages of organoid development, until approximately day 40, with a subsequent decrease when mature neurons emerge (MAP2+ cells, Microtubule-associated protein 2) (day 50, Fig.2a). We found *ZBTB16* enriched in the apical and basal side of the VZ, mainly expressed by progenitor cells (SOX2+ cells, SRY-Box Transcription Factor 2) and not expressed by mature neurons (MAP2+) (Fig. 2c), resembling the RNA expression pattern we observed with the

151 scRNA-seq data (Fig.1i). Thus, *ZBTB16* exhibits a very dynamic expression pattern in hCOs with high protein
152 expression during the initial period of neurogenesis, consistent with data reported from human fetal cortex
153 (Extended data Fig.3c).

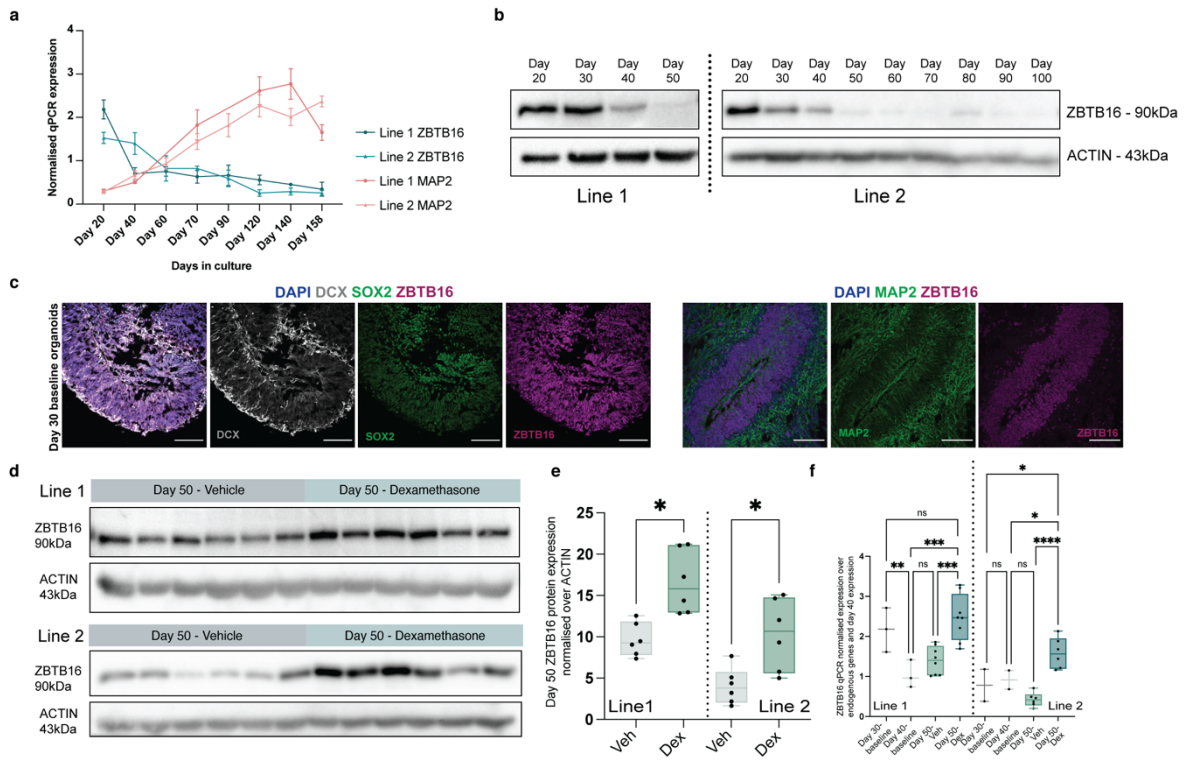

154
155 **Figure 2l Glucocorticoids alter the expression profile of *ZBTB16*. a,** qPCR results (mean +/- SEM) for ZBTB16 and MAP2 in
156 hCOs of different developmental stages. **b,** Western blots of ZBTB16 and ACTIN proteins in hCOs of different developmental
157 stages. **c,** Representative images of day 30 baseline hCOs stained for the immature neuron marker DCX, the progenitor marker
158 SOX2, the mature neuronal marker MAP2, ZBTB16 and the nuclear marker DAPI Scale bars, 100µm. **d,** Western blots of ZBTB16
159 and ACTIN proteins in hCOs treated with 100nM of dex at day 43 and analysed 7 days later at day 50. **e**, Quantification of the
160 effect of 100nM 7 days dex treatment on ZBTB16 protein expression in day 50 hCOs normalized over ACTIN. **f,** qPCR plot for
161 ZBTB16 mRNA expression in hCOs and expression at days 30-50, with vehicle and dex condition at day 50. qPCR, quantitative
162 polymerase chain reaction; hCOs, human cerebral organoids; Veh, vehicle; Dex, dexamethasone. For **e** significance was tested
163 with two tailed Mann-Whitney comparison between treatment and vehicle. For **f** significance was tested with one-way ANOVA
164 with Benjamini, Krieger and Yekutieli multiple testing correction (p= 0.0003, F= 10.39, DF= 3). Mann-Whitney p-values for e or
165 post-hoc p-values for f: **** <=0.0001, *** <=0.001, ** <=0.01, * <=0.05, ns >0.05
166

167 Next, we examined the levels of ZBTB16 expression after dex administration in hCOs (100nM dex, for 7 days
168 starting at day 43- Extended data Fig.4a). Treatment with dex resulted in increased *ZBTB16* expression at the RNA
169 (Extended data Fig.4b) and protein level (Fig.2d,e) in the progenitor cells that line the VZ (Extended data Fig.4c,d).
170 In fact, dex alters the tightly-regulated developmental expression pattern of this TF by reversing its levels to those
171 of day 30 and younger hCOs (Fig.2f). Together, these results suggest that dex maintains high *ZBTB16* expression
172 during later stages of neurogenesis, at developmental time-windows with physiologically lower levels of this TF.
173

174 ***ZBTB16* mimics the effects of glucocorticoids on basal progenitors**

175 To test whether the effect of dex on BPs is mediated via *ZBTB16*, we overexpressed ZBTB16 and GFP from a
176 bicistronic plasmid or GFP from a monocistronic control plasmid, in hCOs starting at day 43 when ZBTB16
177 expression is already declining (Fig.2a,b). Subsequent analyses were performed 7 days after the electroporation,

178 at day 50 (Fig.3a). In order to explore effects on progenitor subtypes of the VZ and the SVZ and on neurons of the
179 CP, we divided the electroporated area in three bins of equal height and analysed the effects of ZBTB16
180 overexpression on GFP+ electroporated cells.
181 ZBTB16 overexpression led to increased numbers of Ki-67+ cells (Fig. 3b,c), indicating an increase in proliferation
182 potential. In analogy to the experiments with dex, we next co-analyzed PAX6 and EOMES expression. Indeed,
183 ZBTB16 overexpression led to a similar phenotype to that of dex, with an overall 25.7% increase in PAX6+EOMES+
184 BPs (Fig. 3d,e) in bins B and C (Fig.3f, 23.8% increase in bin B and 43.1% increase in bin C), which reflect the
185 basal parts of the VZ, the SVZ and the CP. Interestingly, there was a substantial increase of these BPs in bin C
186 (43.1%) which associates to the CP of the organoids, pointing to a potential identity change of this bin to resemble
187 an area with cells typically found in the inner and outer SVZ of gyrencephalic species. In addition, we also found
188 more layer V neurons with ZBTB16 overexpression (BCL11B-positive cells, BAF Chromatin Remodeling Complex
189 Subunit- also known as CTIP2, show a 14% increase, Extended data Fig. 5a,b) indicating increased neuronal
190 production. The birth of these neurons, however, is potentially delayed as they are still migrating and have not yet
191 reached their final destination in bin C (Extended data Fig. 5c, 11.2% more BCL11B+GFP+ cells in bin A and 8.1%
192 less BCL11B+GFP+ cells in bin C). Thus, ZBTB16 overexpression increases the amount of double-positive BPs
193 and of later-born neurons, effects that resemble the ones of dex (Fig.1c-g).

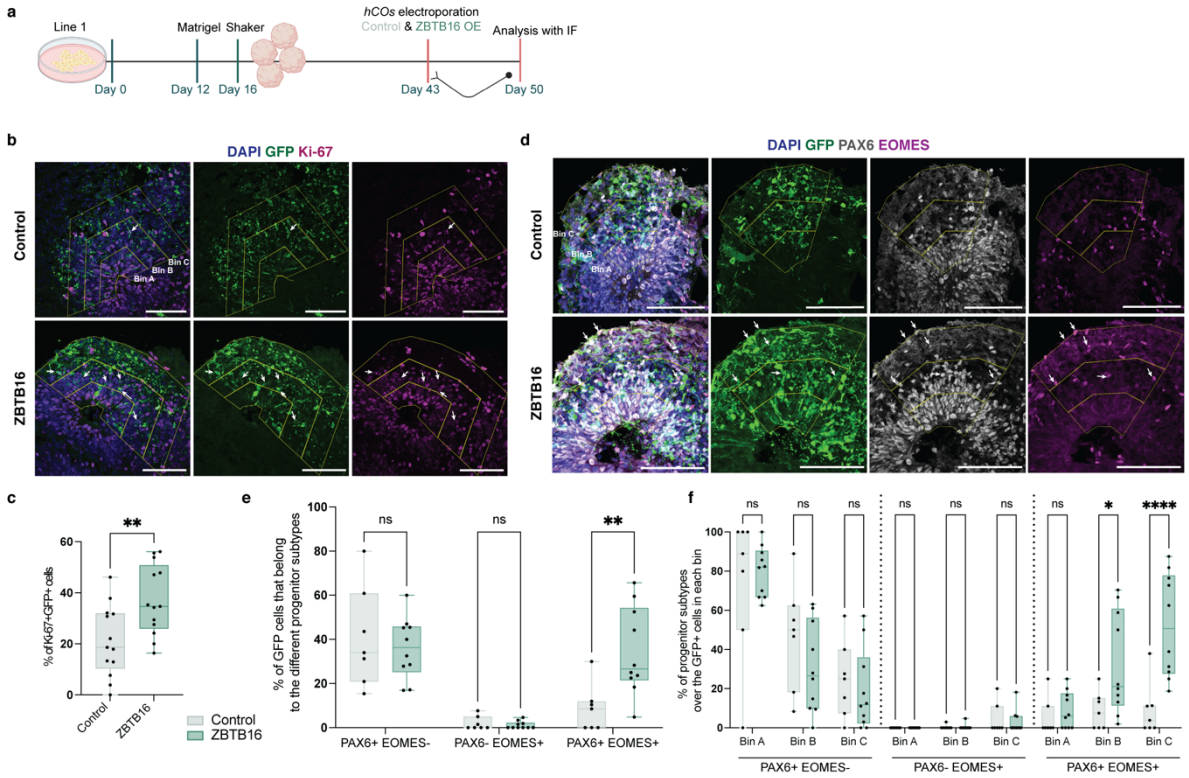

194
195 **Figure 3l *ZBTB16* increases PAX6+EOMES+ basal progenitors in human cerebral organoids. a,** Schematic of Line 1-derived
196 hCOs electroporations and analysis workflow for ZBTB16 OE. **b,** Representative images of day 50 hCOs at control and ZBTB16
197 OE conditions stained for Ki-67, GFP and DAPI. White arrows indicate GFP cells that express Ki-67; Scale bars, 100µm. **c,**
198 Quantification of the total number of GFP cells that are Ki-67 positive normalized over total GFP cells. **d,** Representative images
199 of day 50 hCOs at control and ZBTB16 OE conditions stained for PAX6, EOMES, GFP and DAPI. Arrows indicate GFP cells that
200 co-express PAX6 and EOMES; Scale bars, 100µm. **e,** Quantification of the GFP cells belonging in each progenitor subtype
201 normalized by total GFP cells. **f,** Quantification of the GFP cells belonging in the different single positive progenitor subtypes in
202 each bin and condition normalized by total GFP cells of each bin. hCOs, human cerebral organoids; OE, overexpression; IF,
203 Immunofluorescence. For **c** significance was tested with two tailed Mann-Whitney comparison between ZBTB16-overexpression

204 and control plasmid. For **e&f** significance was tested with two-way ANOVA with Benjamini, Krieger and Yekutieli multiple testing
205 correction (e: p.interaction= 0.0069, F= 5.5, DF= 2/ f: p.interaction = 0.0002, F= 4.17, DF= 8). Mann-Whitney p-values for c or
206 post-hoc p-values for e&f: **** <=0.0001, ** <=0.01, * <=0.05, ns >0.05
207

208 ***ZBTB16* is necessary for the glucocorticoid effects on basal progenitors**

209 In view of the similarity of the dex and ZBTB16 overexpression phenotypes on BPs, we sought to determine whether
210 ZBTB16 is in fact necessary for the dex-induced phenotype. To achieve this, we used CRISPR-Cas9 to knock-out
211 (KO) exon 2 of the *ZBTB16* locus in the Line 2- iPSCs. Exon 2 encodes for more than 50% of the protein and
212 includes the initiating ATG, the BTB/POZ domain and the first two zinc fingers of the binding domain[25]. We created
213 heterozygous Line 2- (from now on called ZBTB16$^{+/-}$) iPSCs where one allele of the *ZBTB16* locus is wild-type and
214 one allele has exon 2 excised. A full KO of exon 2 in both alleles was not viable at the iPSC cell stage. We then
215 treated ZBTB16$^{+/+}$- derived (CRISPR control Line 2- iPSCs) and ZBTB16$^{+/-}$-derived day 43 hCOs with 100nM dex
216 for 7 days and analysed ZBTB16 protein expression as well as the relative abundance of PAX6+EOMES-, PAX6-
217 EOMES+ and PAX6+EOMES+ progenitor subtypes with FCa at day 50 (Fig.4a).

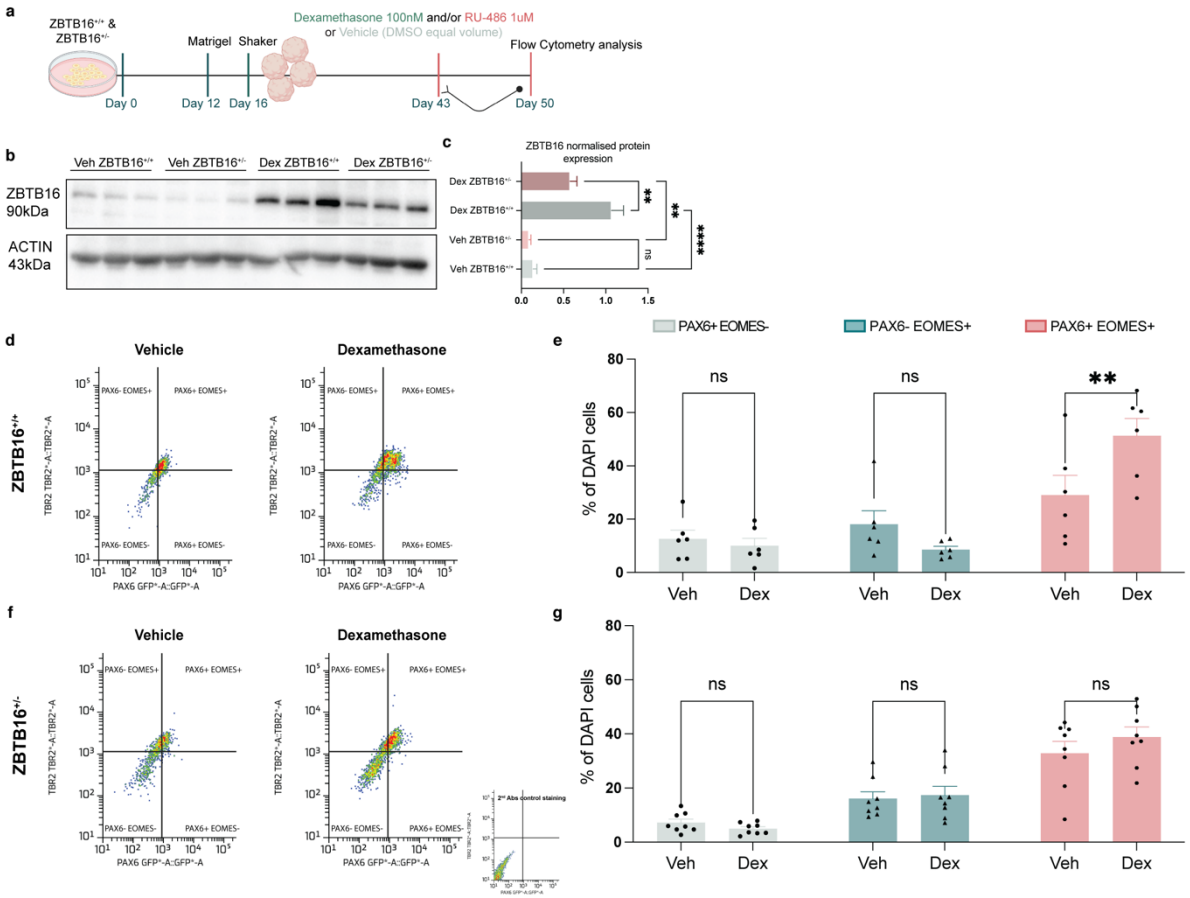

218
219 **Figure 4l *ZBTB16* mediates the effects of glucocorticoids on PAX6+EOMES+ basal progenitors. a,** Treatment paradigm
220 and analysis workflow in hCOs derived from edited Line 2- iPSCs either with ZBTB16$^{+/+}$ or ZBTB16$^{+/-}$ genotypes. **b,** Western blots
221 for ZBTB16 and ACTIN proteins in ZBTB16$^{+/+}$ or ZBTB16$^{+/-}$ derived hCOs at different treatment conditions. **c,** Quantification of the
222 Western blot results for ZBTB16 normalized over ACTIN. **d,** Representative images of FCa of ZBTB16$^{+/+}$-derived hCOs per dex
223 treatment condition. TBR2 is an alternative name for EOMES. **e,** Quantification of the FCa results. Percentages of DAPI cells in
224 each progenitor subtype and treatment condition. **f,** Representative images of FCa analysis of ZBTB16$^{+/-}$-derived hCOs per
225 treatment condition. **g,** Quantification of the FCa results. Percentages of DAPI cells in each progenitor subtype and treatment
226 condition. DMSO, dimethyl sulfoxide; hCOs, human cerebral organoids; Veh, vehicle; Dex, dexamethasone; FCa, flow cytometry
227 analysis. For **c,e&g** significance was tested with two-way ANOVA with Benjamini, Krieger and Yekutieli multiple testing correction

228 (c: p.interaction = 0.03, F= 6.6, DF= 1/ e: p.interaction = 0.0068, F= 5.9, DF= 2/ g: p.interaction = 0.97, F= 0.38, DF= 2). Post-hoc
229 p-values: ** <=0.01, ns >0.05
230
231 ZBTB16$^{+/-}$ hCOS showed significantly less increase of the ZBTB16 protein following dex treatment than the
232 ZBTB16$^{+/+}$ hCOs (46% less increase, Fig.4b,c). FCa of the ZBTB16$^{+/+}$ hCOs validated the increase of
233 PAX6+EOMES+ BPs under dex treatment (Fig.4d,e- 22.2% increase, similar to the increase found with the Line 2
234 wild-type hCOs (Extended data Fig. 2b,c). However, in the ZBTB16$^{+/-}$ hCOs, the number of double-positive BPs
235 was not significantly increased in the dex condition in respect to veh (Fig.4f,g- 6% non-significant increase).
236 Together, these results indicate that ZBTB16 is necessary for the effects of GCs on PAX6+EOMES+ BPs and
237 suggests that it could potentially play a key role in the maintenance of the PAX6+EOMES+ BP population in gyrified
238 species under baseline conditions.
239
240 **Heterochronic *ZBTB16* expression in mouse fetal brain is sufficient to induce basal progenitors typically**
241 **enriched in gyrified species**
242 While the principles of neurogenesis are similar among all mammalian species, differences exist in respect to their
243 temporal progression as well as to the different progenitor subtypes populating the SVZ which play a key role in the
244 overall neurogenic potential. In lissencephalic species BPs double-positive for PAX6 and EOMES are very rare[16],
245 the neurogenic period is much shorter[26] (9 days in mice compared to 110 days in humans) and *ZBTB16* is not
246 physiologically expressed at any point during the neurogenic period (Extended data Fig.3a,b). In order to analyse
247 if altered expression of *ZBTB16* during neurogenesis would lead to increased numbers of PAX6+EOMES+ BPs
248 also in a lissencephalic species, we performed *in utero* electroporations at E13.5 in mouse brains with the same
249 plasmids as for the hCOs and analysed the effects of human *ZBTB16* overexpression at E16.5 (Fig.5a). Considering
250 the more complex cortical cellular architecture of the mouse brain as compared to hCOs, we divided the
251 electroporated area in five bins of equal height where bin A includes the VZ and the SVZ, bin B the SVZ and
252 intermediate zone (IZ), bin C the IZ and bins D and E the CP.
253 In mice, ZBTB16 overexpression significantly changed the distribution of the GFP+ electroporated cells.
254 ZBTB16+GFP+ cells accumulated in the SVZ with less cells reaching the outer-most part of the cortical plate
255 (Fig.5b,c), indicating possible identity changes and/or altered timing of differentiation. Similar to hCOs, we found
256 more Pax6+Eomes+ BPs (Fig.5d,e, 8.8% overall increase) in bin A and bin B (Fig. 5f, 16.5% increase in bin A and
257 11.8% increase in bin B). Interestingly, in mice, Pax6-Eomes+ IPs, which are the vast majority of endogenous BPs
258 of lissencephalic species[16], were significantly decreased after ZBTB16 overexpression (Fig.5e,f, 10.6% decrease
259 in bin A and 15.1% decrease in bin B). Our results thus suggest that ZBTB16 overexpression in lissencephalic
260 neurogenesis leads to increased gyrified species-enriched BPs at the expense of the endogenous neurogenic
261 progenitors.
262 As discussed, the double-positive BPs have a higher proliferative potential which contributes to the higher
263 abundance of neurons in gyrified species[16,17]. This seems to also translate to lissencephalic species where
264 physiologically these BPs are very rare. Here, we also found that ZBTB16 overexpression led to increased numbers
265 of deep layer V neurons expressing Bcl11b (33.3% increase, Fig.5g,h) and layer VI neurons expressing Tbr1 (T-
266 box brain transcription factor 1, 4.3% increase, Extended data Fig.6a,b) but not of upper layer IV neurons that
267 express Satb2 (SATB Homeobox 2, Extended data Fig.6d,e), supporting the increased neurogenic potential of
268 these gyrencephalic BPs also in other species. When examining the distribution of neurons, we found an
269 accumulation in the SVZ- and IZ- areas with less neurons having reached the CP after ZBTB16 overexpression
270 (Fig.5i & Extended data Fig.6c,f). This finding again lends support to the fact that the higher proliferative capacity
271 of the PAX6+EOMES+ BPs associates with a potentially longer neurogenic period similar to what we observed

following dex treatment and ZBTB16 overexpression in hCOs. In fact, when analyzing the distribution of neurons across the five bins not 3 but 6 days post electroporation (i.e. at day E19.5/birth) there were no significant differences for the distribution of cells with ZBTB16 overexpression (Extended data Fig.6g-k), indicating that migratory processes are probably not affected.

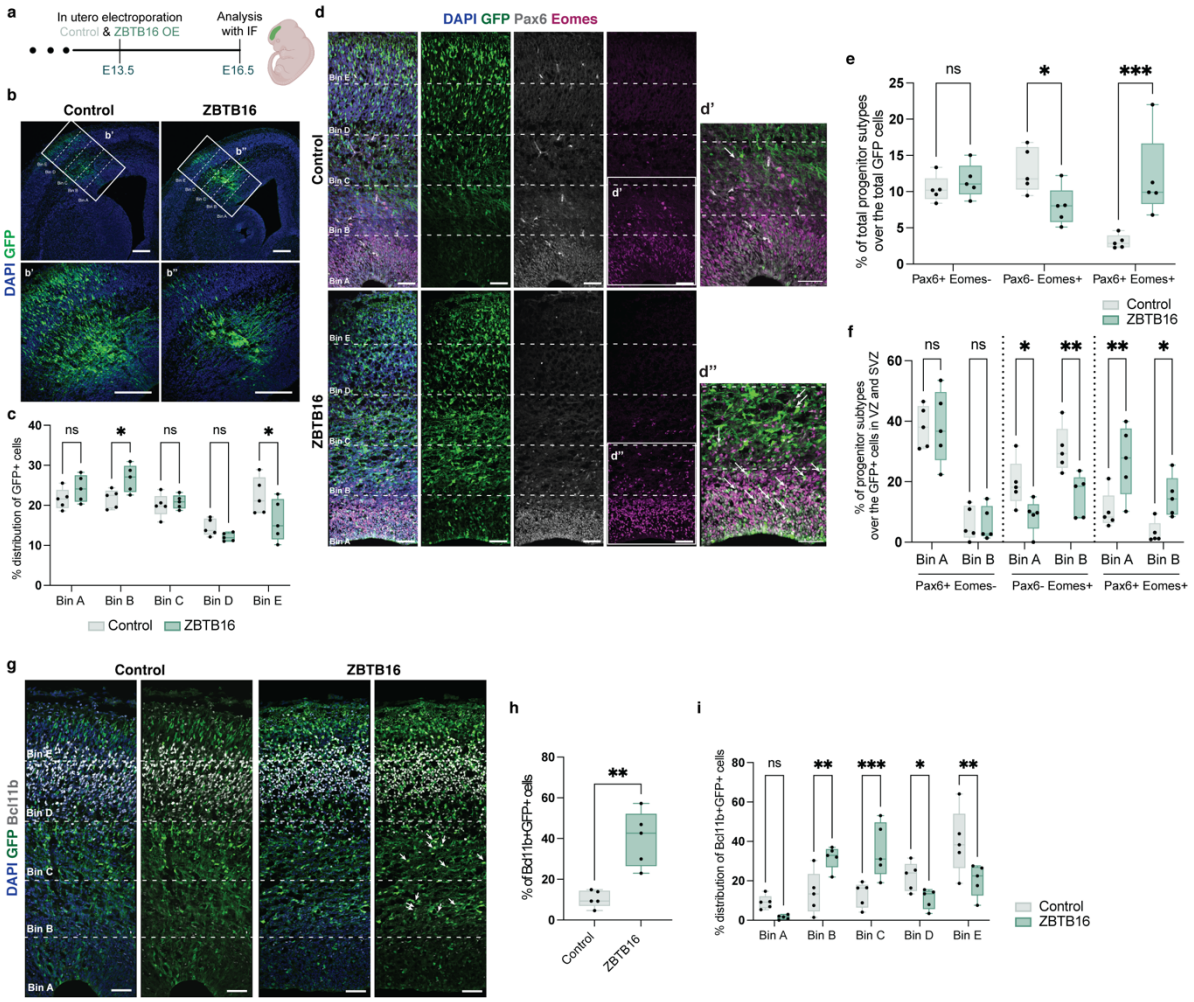

Figure 5l *ZBTB16* increases PAX6+EOMES+ basal progenitors and deep layer neurons in a lissencephalic species. a, Workflow of the *in utero* electroporations of *ZBTB16* and analysis in fetal mice. **b,** Representative images of E16.5 fetal mouse brains at control and ZBTB16 OE conditions stained for GFP and DAPI. Box indicates the electroporation areas and **b', b''** are zoom-ins; Scale bars, 100µm. **c,** Quantification of the distribution of GFP cells in each bin normalized by the total number of GFP cells. **d,** Representative images of E16.5 fetal mouse brains at control and ZBTB16 OE conditions stained for Pax6, Eomes, GFP and DAPI. **d' and d''** are zoom-ins. Arrows indicate GFP cells that co-express Pax6 and Eomes; Scale bars, 50µm. **e,** Quantification of the GFP cells belonging in the different progenitor subtypes normalized by total GFP cells. **f,** Quantification of the GFP cells belonging in the different positive progenitor subtypes in each bin normalized by total GFP cells of each bin. **g,** Representative images of E16.5 fetal mouse brains at control and ZBTB16 OE conditions stained for the layer V neuronal marker Bcl11b, GFP and DAPI. Arrows indicate GFP cells that express Bcl11b; Scale bars, 50µm. **h,** Quantification of the GFP cells that are Bcl11b+ normalized by total GFP cells. **i,** Quantification of the distribution of Bcl11bB+GFP+ cells in each bin normalized by total number of Bcl11b+GFP+ cells. OE, overexpression; IF, Immunofluorescence. For **h** significance was tested with two tailed Mann-Whitney comparison between ZBTB16-overexpression and control plasmid. For **c,e,f&i** significance was tested with two-way ANOVA with Benjamini, Krieger and Yekutieli multiple testing correction (c: p.interaction = 0.003, F= 4.7, DF= 4/ e: p.interaction = 0.0003, F= 11.84, DF= 2/ f: p.interaction < 0.0001, F= 6.58, DF= 5/ i: p.interaction < 0.0001, F= 10.66, DF= 4). Mann-Whitney p-values for h or post-hoc p-values for c,e,f&i: *** <=0.001, ** <=0.01, * <=0.05, ns >0.05

294 ***ZBTB16* directly induces *PAX6* expression**

295 Considering that dex via *ZBTB16* seems to sustain *PAX6* expression in EOMES+ cells, even in a lissencephalic
296 species where physiologically they are mutually exclusive[27–29], and that *ZBTB16* is a TF, we analysed the activatory
297 capacity of ZBTB16 on *PAX6* human promoters. *PAX6* has three promoter regions that regulate tissue-specific
298 expression and that are highly conserved between humans and rodents: the P0, P1 and Pa promoters [30,31]
299 (Extended data Fig. 7a). Using luciferase assays, we found that ZBTB16 activates the P1 promoter of *PAX6* but
300 not the P0 and Pa promoters (Extended data Fig.7b). This suggests that ZBTB16 could regulate *PAX6* expression
301 via the P1 promoter which is active during neocortical development, in comparison to the P0 and Pa promoters
302 which are minimally active[30]. This could be a potential mechanism responsible for sustaining *Pax6* expression in
303 Eomes+ cells even in mice by ZBTB16 overexpression circumventing the negative feedback loop that
304 physiologically ensures that *Pax6* and *Eomes* are not co-expressed in rodents[27–29].
305

306 **Glucocorticoids interact with the *ZBTB16* genetic and epigenetic landscape**

307 In order to analyse the mechanisms via which the physiological temporal expression pattern of ZBTB16 is affected
308 by GCs, we looked at the gene regulatory landscape of the human *ZBTB16* locus in response to GCs. ENCODE
309 data indicate the existence of intronic GR-response elements (GREs) at the human *ZBTB16* locus (Fig.6a). We
310 have previously shown that activation of GR leads to DNA methylation changes in GREs of target genes which
311 associates with changes in gene transcription[32,33]. To identify the molecular mechanism by which dex via GR
312 induced *ZBTB16* expression, we treated day 30 hCOs with 100nM dex for 7 days and used HAM-TBS[34] (Highly
313 Accurate Method for Targeted Bisulfite Sequencing) to measure DNA methylation of all GREs, as identified by
314 public GR-ChIP sequencing datasets (Extended data Table 3) and additional non GR-related GREs (Fig.6a). Out
315 of 55 CpGs covered in this assay, 36 were located within GREs and 19 in enhancer elements lacking GR binding
316 sites. While only 1 of the CpGs outside these GR-binding regions showed significant DNA methylation level changes
317 following dex stimulation (Extended data Table 4), this was true for 18 of the 36 CpGs around GREs (Fig.6b and
318 Extended data Table 4). All significantly altered GRE-CpGs are located in enhancer regions that loop to the
319 transcriptional start site of *ZBTB16* ("GeneHancer" track in Fig.6a and Bothe *et al.*, Life Science Alliance, 2021[35]).
320 Our data thus support a model in which GR binds to these enhancer elements as evidenced by altered DNA
321 methylation and increases ZBTB16 transcription.

322 Knowing that environmental factors, including GCs, can interact with the genetic landscape to modulate their effects
323 on expression[36], we next analysed the genetic landscape of *ZBTB16*. We catalogued the SNPs (single nucleotide
324 polymorphisms) in the *ZBTB16* locus previously associated with neurobehavioral and brain structural outcomes
325 (GWAS Catalogue & Extended data Table 5) and identified rs648044 as the only variant associated with both
326 (Extended data Table 6). rs648044 has been associated with educational attainment in two GWAS (genome-wide
327 association study) for this trait (Lee *et al.*[37]: N= 1,131,881, FDR = $9*10^{-9}$ & Okbay *et al.*[38]: N= 3,037,499, FDR =
328 $2*10^{-8}$) and with generalized cortical thickness[39] (N= 35,657 individuals, FDR = $6*10^{-9}$). In the latter GWAS on
329 cortical morphology, gene-level analysis also identified the whole *ZBTB16* locus to be significantly associated with
330 generalized cortical surface area (FDR = $7.2*10^{-14}$) and thickness (FDR = $1.9*10^{-8}$), thus suggesting relevance of
331 *ZBTB16* for adult cortical morphology. In addition, rs648044 is located within the responsive GR-enhancer area
332 identified with the DNA methylation analysis (Fig.6a), pointing to a possible role of this SNP in GC-regulation of
333 *ZBTB16* transcription.

334 We first analysed whether this SNP moderates dex-induced activity of the surrounding 200 bp (base pair) enhancer
335 element using a STARR-qPCR (Self Transcribing Active Regulatory Region- qPCR) approach. We identified that
336 the sequence surrounding rs648044 indeed possesses enhancer activity that is increased with GR activation via
337 dex (Extended data Fig.8a). The extent of the dex-induced activity increase was rs648044 allele-dependent, with

338 the allele associated with higher educational attainment (A-allele), conferring a significantly stronger increase
339 following dex (Extended data Fig.8b). Next, we used CRISPR-Cas9 to KO 400 nucleotides surrounding rs648044
340 in Line 2- iPSCs in order to identify whether this enhancer affects *ZBTB16* transcription in hCOs. The rs648044
341 genotype of Line 2- iPSCs is heterozygous (G/A), with the rarer A allele (allele frequency = 0.35) creating a
342 degenerated partial GR binding site (described half site[40]: AGXACAG, rs648044 creates: AGCAGAG, Extended
343 data Fig.8c). A KO of the A allele resulted in rs648044$^{G/-}$ cells that only carry the G allele (Extended data Fig.8c).
344 Using the edited cell line (rs648044$^{G/-}$) and the control cell line carrying both alleles (rs648044$^{G/A}$), we found that
345 the absence of the A allele confers significantly less induction of *ZBTB16* following 100nM dex in day 30 hCOs
346 treated for 7 days (Extended data Fig.8d), suggesting that the enhancer containing rs648044 modulates dex-
347 mediated transcriptional effects on *ZBTB16* in hCOs.

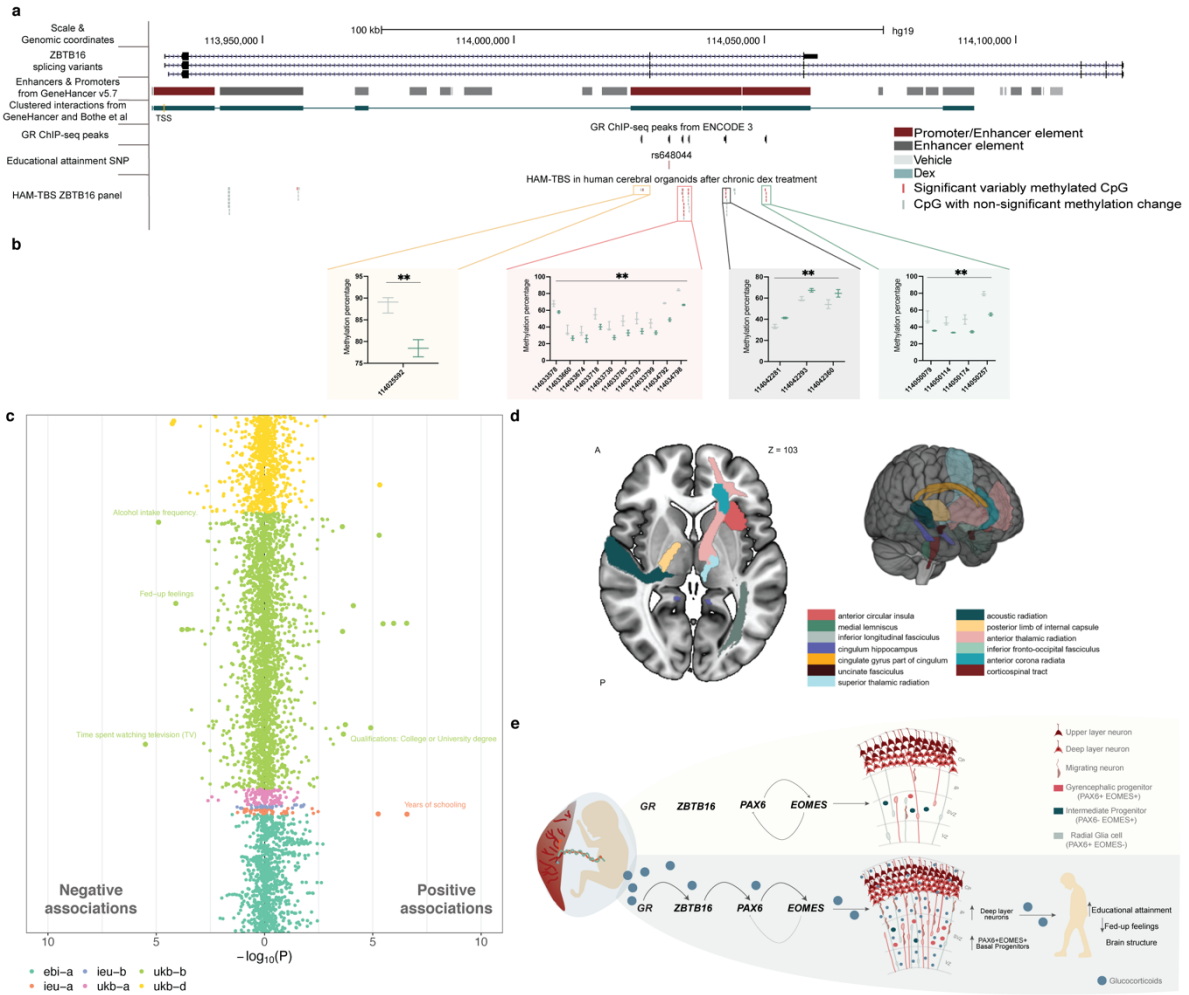

348
349 **Figure 6l Glucocorticoids interact with the genetic and epigenetic landscape of ZBTB16 to impact postnatal**
350 **neurobehavioral and structural phenotypes. a,** Graphical representation of the ZBTB16 locus including the position of the
351 amplicon for HAM-TBS. **b,** HAM-TBS results for CpGs with significantly altered DNA methylation levels following exposure to 7
352 days of 100nM dex vs. vehicle. **c,** Plot depicting Phe-WAS-MRa associations as -log of the p-value for rs648044 with various
353 phenotypes from the UK Biobank. Single phenotypes are depicted as individual points. Associations are presented based on
354 negative (negative MRa estimate.i.e. lower quantitative measures with A-allele effects) and positive (positive MRa estimate, i.e.
355 higher quantitative measures with A-allele effects) effects. Color coding reflects the different sources of GWAS depicted in the
356 legend. Traits that remain significant following Benjamini-Hochberg correction are shown with larger dots and are listed in
357 Extended data Table 8. All neurobehavioral traits are labeled. **d,** Illustration of significant MRa associations between brain imaging
358 phenotypes and rs648044 mapped onto the brain atlases. All effects are listed also in Extended data Table 9. **e,** Summary of the
359 effects of glucocorticoids on ZBTB16 expression, cortical cellular architecture during development and postnatal phenotypes. GR,

glucocorticoid receptor; ChIP, chromatin immunoprecipitation; Seq, sequencing; SNP, single nucleotide polymorphism; HAM-TBS, highly accurate method for targeted bisulfite sequencing; Dex, dexamethasone; MRa, mendelian randomization analysis. For **b** significance was tested with two-way ANOVA with Benjamini, Krieger and Yekutieli multiple testing correction (GH11J114152 enhancer: p.treatment < 0.0001, F= 7.33, DF= 31/ GH11J114174 enhancer: p.treatment< 0.0001, F= 37.32, DF= 3). Post-hoc p-values: ** <=0.01

Glucocorticoids x rs648044 effects on *ZBTB16* relate to beneficial postnatal outcomes

Given the functional effects of rs648044 on GC-induced ZBTB16 expression in the developing cortex, we used phenome-wide mendelian randomization analysis (MRa-PheWAS) to identify causal effects of *ZBTB16* levels on 7,323 phenotypes from the UK Biobank and the NHGRI-EBI GWAS Catalog (Extended data Table 7) that include, among many others, neurobehavioral traits and adult neuroimaging data. We used rs648044 as exposure and the magnitude of the allele-specific expression changes following dex in the STARR-qPCR experiment as instrument to test for these associations. MRa-PheWAS provided strong evidence for associations with multiple outcomes as indicated by the QQ-plot (Extended data Fig.8f). MRa on various phenotypes, including endophenotypes and diseases (N= 4,360), showed significant associations of GC-altered *ZBTB16* expression with 22 phenotypes after multiple testing correction. These included positive associations with years of schooling and whether individuals had obtained a college or university degree (Fig.6c and Extended data Table 8), which are direct measures of educational attainment. This supports the idea that the functional effects of rs648044 on GC-induced *ZBTB16* transcription in the developing cortex, are putatively causally-related to educational attainment postnatally. In addition, GC-induced *ZBTB16* transcription was negatively associated with “fed-up feelings” a phenotype related to neuroticism[41], “alcohol intake” and “time spent watching television” (Fig.6c), suggesting associations of higher *ZBTB16* levels with beneficial postnatal outcomes and decreased associations with negative outcomes (Fig.6c). Given the previously published relationships of both educational attainment[42–45] as well as rs648044[37–39] with cortical volumes and white matter measures, we also ran an MRa-PheWAS on all neuroimaging phenotypes (N = 3,143) in the UK Biobank using the same instrument. We observed 21 significant associations after multiple testing correction (Fig.6d, Extended data Fig.8g and Extended data Table 9). Most evidence indicated that GCs x rs648044-mediated increases in *ZBTB16* expression were significantly associated with altered white matter measures and with higher anterior circular insula thickness (Fig. 6d). Thus, higher GC-induced *ZBTB16* expression in rs648044 A allele carriers is associated with higher educational attainment and increased cortical thickness as well as altered white matter measures postnatally. This suggests that the genetic association of this variant with adult neurobehavioral and brain structural measures could be mediated in parts by its effects on GC-induced *ZBTB16* levels in early brain development and in consequence their effects on neurogenesis.

Discussion

With this work we sought to understand the effects of GC excess during human cortical neurogenesis at the cellular and molecular level. We found that GCs increase a particular population of neural progenitor cells that co-express PAX6 and EOMES. These progenitor cells were found at the basal side of the germinal zones and are known to be enriched in species with gyrified brains related to a higher proliferative capacity, thus contributing to increased neuronal production[16,17,46]. We show that these effects of GCs are mediated by an alteration of the developmental expression profile of a TF called *ZBTB16*. *ZBTB16* activates a forebrain active promoter of *PAX6*, potentially explaining how GCs increase the numbers of PAX6+EOMES+ BPs. The increase in these specific BPs is followed by increased numbers of deep layer neurons and may relate to beneficial postnatal outcomes at the neurobehavioral level, like increased education attainment, and altered brain structure (Fig.6e).

Precise temporal and spatial regulation of gene expression by TFs is key for the proper unfolding of neurogenic processes[22]. Thus, we focused on GC-effects on TFs as the potential molecular mechanism responsible for their

404 effects on neurogenesis. We showed that GCs alter the tightly regulated developmental expression profile of a TF
405 called *ZBTB16* in hCOs which in turn mediates the GC-effects on neurogenesis. While ZBTB16 shows a dynamic
406 expression pattern in both gyrencephalic and lissencephalic species, the expression among species differs
407 according to developmental time-windows. In mice, *Zbtb16* appears at E7.5 in the neuroectoderm, increases until
408 E10.5 and is subsequently downregulated and finally only expressed in specific areas of the hindbrain and the
409 septum but not the forebrain[24], so that in rodents *Zbtb16* is not expressed during cortical neurogenesis. This is
410 contrary to the expression pattern observed in human fetal brain and hCOs (Extended data Fig.3), where *ZBTB16*
411 is expressed during the initial stages of neurogenesis. This points to possible divergent actions of this TF in
412 gyrencephalic and lissencephalic species neurodevelopment and highlights this protein as important for gyrified-
413 species enriched neurogenic processes at baseline as well as in response to GCs.
414 Indeed, overexpressing ZBTB16 in the mouse fetal brain during the neurogenic period (E13-E16, when *Zbtb16* is
415 not anymore expressed physiologically) leads to increased Pax6+Eomes+ BPs. In lissencephalic cortical
416 development *Pax6* and *Eomes* create a positive feedforward cascade that self-regulates with direct negative
417 feedback effects[27–29], ensuring mutually exclusive expression of these proteins. This seems to be overridden by
418 asynchronous overexpression of *ZBTB16*. We also show that *ZBTB16* directly activates the *PAX6* promoter P1[30],
419 that is functional in the forebrain, and sustains PAX6 expression potentially leading to the increased
420 PAX6+EOMES+ BPs both in hCOs and in mice. Thus, via the action of *ZBTB16,* GCs have the ability to extend or
421 open a sensitive developmental time-window for the production of gyrencephalic-enriched BPs in a lissencephalic
422 species resulting in enhanced neurogenic potential with higher production of deep layer neurons.
423 Given the high prevalence of premature births, GC excess during human neurodevelopment through administration
424 of sGCs is a very common phenomenon[9]. In fact, yearly in about ~615,000 extreme preterm pregnancies sGC
425 treatments would take place in a period of active neurogenesis, before GW28[10,13]. While endogenous GCs are
426 important for the maturation and function of fetal organs[1], prenatal excess of GCs has been extensively associated
427 with long-term metabolic, endocrine and cardiovascular problems[6] and risk for neurodevelopmental[47] and mental[48]
428 disorders in the offspring. Evidence from a recent meta-analysis of studies including more than 1,25 million children
429 re-affirms the association of exposure to sGCs with negative effects on cognitive and neuropsychiatric outcomes
430 when administered to children with late-preterm or term birth. However, the authors also report a significantly lower
431 risk for neurodevelopmental impairments in children with extremely preterm birth (<28 GWs), that were treated with
432 sGCs between GW22 to GW27[3]. This meta-analysis could be pointing to potential differential effects of GCs on
433 neurodevelopment depending on the developmental time-window they were administered in.
434 One process that is different among extremely preterm and term or adult brains and might contribute to these
435 dichotomous effects is human cortical neurogenesis, which peaks ~GW20 and is reduced but present until GW28
436 in the SVZ of the brain[13]. This means that extremely preterm born children are still treated within the time window
437 of active cortical neurogenesis. Such differential effects are supported by a study in mice in which dex administration
438 during neurogenesis was associated with anxiolytic and anti-depressive like behavior in the adult offspring[49] while
439 increased, prolonged exposure to GCs following completion of cortical neurogenesis has repeatedly been
440 associated with increased anxiety and depressive-like behaviors and decreased cognitive ability in these animals[50].
441 With this work we highlight a potential molecular and cellular pathway for the lasting effects of prenatal sGC
442 exposure during neurogenesis and pinpoint *ZBTB16* as an important hub gene mediating GCs effects on cortical
443 neurogenesis and potentially postnatal phenotypes. The latter is supported by results from an MRa-PheWAS where
444 we find potentially causal associations of GC-altered *ZBTB16* levels in neurodevelopment with higher educational
445 attainment, lower neuroticism measures and altered cortical and white matter measures.
446 Overall, our work provides a molecular and cellular mechanism of how GCs administered early in development,
447 during the neurogenic period, affect the cytoarchitecture of the developing cortex which in turn associates with

postnatal outcomes at the brain structural but also neurobehavioral level. This work highlights how an environmental factor can affect brain development and postnatal health and underscores the importance of taking the developmental time-window into account when studying prenatal exposures. In addition, the new knowledge provided potentially explains the associations of early sGC use with beneficial behavioral and neurodevelopmental measures found in the literature and, thus, may help refine sGC treatment guidelines according to the stage of pregnancy they are administered in.

References

1. Carson, R., Monaghan-Nichols, A. P., DeFranco, D. B. & Rudine, A. C. Effects of antenatal glucocorticoids on the developing brain. *Steroids* **114**, 25–32 (2016).
2. Committee on Obstetric Practice. Antenatal Corticosteroid Therapy for Fetal Maturation. *Obstetrics and Gynecology* **130**, 102–109 (2017).
3. Ninan, K., Liyanage, S. K., Murphy, K. E., Asztalos, E. V & McDonald, S. D. Evaluation of Long-term Outcomes Associated With Preterm Exposure to Antenatal Corticosteroids: A Systematic Review and Meta-analysis. *JAMA pediatrics* e220483 (2022). doi:10.1001/jamapediatrics.2022.0483
4. Mcewen, B. S. *et al.* Mechanisms of stress in the brain. *Nature Neuroscience* **18**, (2015).
5. Barker, D. J. P. The developmental origins of chronic adult disease. *Acta Paediatr Suppl* 26–33 (2004). doi:10.1080/08035320410022730
6. Monk, C., Lugo-Candelas, C. & Trumpff, C. Prenatal Developmental Origins of Future Psychopathology: Mechanisms and Pathways. *Annual Review of Clinical Psychology* **15**, (2019).
7. Krontira, A. C., Cruceanu, C. & Binder, E. B. Glucocorticoids as Mediators of Adverse Outcomes of Prenatal Stress. *Trends in Neurosciences* **43**, 394–405 (2020).
8. Lajic, S., Karlsson, L. & Nordenström, A. Prenatal Treatment of Congenital Adrenal Hyperplasia : Long-Term Effects of Excess Glucocorticoid Exposure. *Hormone Research in Pediatrics* (2018). doi:10.1159/000485100
9. Cao, G., Liu, J. & Liu, M. Global, Regional, and National Incidence and Mortality of Neonatal Preterm Birth, 1990-2019. *JAMA Pediatrics* 1–10 (2022). doi:10.1001/jamapediatrics.2022.1622
10. Chawanpaiboon, S. *et al.* Global, regional, and national estimates of levels of preterm birth in 2014: a systematic review and modelling analysis. *The Lancet Global Health* **7**, e37–e46 (2019).
11. The RECOVERY Collaborative Group. Dexamethasone in Hospitalized Patients with Covid-19 — Preliminary Report. *The New England Journal of Medicine* 1–11 (2020). doi:10.1056/NEJMoa2021436
12. Mcintosh, J. J. Corticosteroid Guidance for Pregnancy during COVID-19 Pandemic. *Americal Journal of Perinatology* 809–812 (2020).
13. Malik, S. *et al.* Neurogenesis continues in the third trimester of pregnancy and is suppressed by premature birth. *Journal of Neuroscience* **33**, 411–423 (2013).
14. Lancaster, M. A. & Knoblich, J. A. Generation of cerebral organoids from human pluripotent stem cells. *Nature Protocols* **9**, 2329–2340 (2014).
15. Cruceanu, C. *et al.* Cell-Type-Specific Impact of Glucocorticoid Receptor Activation on the Developing Brain: A Cerebral Organoid Study. *American Journal of Psychiatry* **179**, 375–387 (2022).
16. Dehay, C., Kennedy, H. & Kosik, K. S. The Outer Subventricular Zone and Primate-Specific Cortical Complexification. *Neuron* **85**, 683–694 (2015).
17. Betizeau, M. *et al.* Precursor Diversity and Complexity of Lineage Relationships in the Outer Subventricular Zone of the Primate. *Neuron* **80**, 442–457 (2013).
18. Romero, C. D. J., Bruder, C., Tomasello, U. & Sanz-anquela, J. M. Discrete domains of gene expression

492 in germinal layers distinguish the development of gyrencephaly. *The EMBO Journal* **34**, 1859–1874 (2015).
493 19. Florio, M. & Huttner, W. B. Neural progenitors, neurogenesis and the evolution of the neocortex.
494 *Development (Cambridge)* **141**, 2182–2194 (2014).
495 20. Matsumoto, N., Tanaka, S., Horiike, T. & Shinmyo, Y. A discrete subtype of neural progenitor crucial for
496 cortical folding in the gyrencephalic mammalian brain. *Elife* 1–26 (2020).
497 21. Borrell, V. & Götz, M. Role of radial glial cells in cerebral cortex folding. *Current Opinion in Neurobiology*
498 **27**, 39–46 (2014).
499 22. Silbereis, J. C., Pochareddy, S., Zhu, Y., Li, M. & Sestan, N. The Cellular and Molecular Landscapes of the
500 Developing Human Central Nervous System. *Neuron* **89**, 248 (2016).
501 23. Liu, T. M., Lee, E. H., Lim, B. & Shyh-Chang, N. Balancing Stem Cell Self-renewal and Differentiation with
502 PLZF. *Stem cells (Dayton, Ohio)* 277–287 (2015). doi:10.1002/stem.2270
503 24. Avantaggiato, V. *et al.* Developmental analysis of murine Promyelocyte Leukemia Zinc Finger (PLZF) gene
504 expression: implications for the neuromeric model of the forebrain organization. *The Journal of*
505 *Neuroscience* **15**, 4927–42 (1995).
506 25. Hai, L., Szwarc, M. M., Lanza, D. G., Heaney, J. D. & Lydon, J. P. Using CRISPR / Cas9 engineering to
507 generate a mouse with a conditional knockout allele for the promyelocytic leukemia zinc finger transcription
508 factor. 1–8 (2019). doi:10.1002/dvg.23281
509 26. Stepien, B. K., Vaid, S. & Huttner, W. B. Length of the Neurogenic Period—A Key Determinant for the
510 Generation of Upper-Layer Neurons During Neocortex Development and Evolution. *Frontiers in Cell and*
511 *Developmental Biology* **9**, 1–20 (2021).
512 27. Manuel, M. *et al.* Controlled overexpression of Pax6 in vivo negatively auto- regulates the Pax6 locus ,
513 causing cell-autonomous defects of late cortical progenitor proliferation with little effect on cortical
514 arealization. *Development* **555**, 545–555 (2007).
515 28. Sansom, S. N. *et al.* The Level of the Transcription Factor Pax6 Is Essential for Controlling the Balance
516 between Neural Stem Cell Self- Renewal and Neurogenesis. *PLoS Genetics* **5**, 20–23 (2009).
517 29. Elsen, G. E., Bedogni, F., Hodge, R. D. & Bammler, T. K. The Epigenetic Factor Landscape of Developing
518 Neocortex Is Regulated by Transcription Factors. *Frontiers in Neuroscience* **12**, (2018).
519 30. Anderson, T. R., Hedlund, E. & Carpenter, E. M. Differential Pax6 promoter activity and transcript
520 expression during forebrain development. *Mechanisms of Development* **114**, 171–175 (2002).
521 31. Tyas, D. A. *et al.* Functional conservation of Pax6 regulatory elements in humans and mice demonstrated
522 with a novel transgenic reporter mouse. *BMC Developmental Biology* **6**, 1–11 (2006).
523 32. Provençal, N. *et al.* Glucocorticoid exposure during hippocampal neurogenesis primes future stress
524 response by inducing changes in DNA methylation. *Proceedings of the National Academy of Sciences* **117**,
525 201820842 (2019).
526 33. Wiechmann, T. *et al.* Identification of dynamic glucocorticoid- induced methylation changes at the FKBP5
527 locus. *Clinical Epigenetics* 1–14 (2019).
528 34. Roeh, S. *et al.* HAM-TBS: High-accuracy methylation measurements via targeted bisulfite sequencing.
529 *Epigenetics and Chromatin* **11**, 1–10 (2018).
530 35. Bothe, M., Buschow, R. & Meijsing, S. H. Glucocorticoid signaling induces transcriptional memory and
531 universally reversible chromatin changes. *Life Science Alliance* **4**, 1–17 (2021).
532 36. Klengel, T. & Binder, E. B. Epigenetics of Stress-Related Psychiatric Disorders and Gene × Environment
533 Interactions. *Neuron* **86**, 1343–1357 (2015).
534 37. Lee, J. J. *et al.* Gene discovery and polygenic prediction from a genome-wide association study of
535 educational attainment in 1.1 million individuals. *Nature genetics* **50**, (2018).

38. Okbay, A. *et al.* Polygenic prediction of educational attainment within and between families from genome-wide association analyses in 3 million individuals. *Nature genetics* **54**, (2022).
39. Makowski, C. *et al.* Vertex-wise multivariate genome-wide association study identifies 780 unique genetic loci associated with cortical morphology. *Neuroimage* 1–19 (2022). doi:10.1016/j.neuroimage.2021.118603.Vertex-wise
40. Schiller, B. J., Chodankar, R., Watson, L. C., Stallcup, M. R. & Yamamoto, K. R. Glucocorticoid receptor binds half sites as a monomer and regulates specific target genes. *Genome Biology* **15**, 1–16 (2014).
41. Smith, D. J. *et al.* Prevalence and Characteristics of Probable Major Depression and Bipolar Disorder within UK Biobank : Cross-Sectional Study of 172 , 751 Participants. **8**, 1–7 (2013).
42. Bartrés-Faz, D. *et al.* Characterizing the molecular architecture of cortical regions associated with high educational attainment in older individuals. *Journal of Neuroscience* **39**, 4566–4575 (2019).
43. Ge, T. *et al.* The Shared Genetic Basis of Educational Attainment and Cerebral Cortical Morphology. *Cerebral Cortex* **29**, 3471–3481 (2019).
44. Kim, J. P. *et al.* Effects of education on aging-related cortical thinning among cognitively normal individuals. *Neurology* **85**, 806–812 (2015).
45. Vaqué-alcázar, L., Sala-llonch, R. & Valls-pedret, C. Differential age-related gray and white matter impact mediates educational influence on elders ' cognition. *Brain Imaging and Behavior* **11**, 318–332 (2017).
46. Garcia, M. T., Chang, Y., Arai, Y. & Huttner, W. B. S-Phase Duration Is the Main Target of Cell Cycle Regulation in Neural Progenitors of Developing Ferret Neocortex. *The Journal of comparative neurology* **470**, 456–470 (2016).
47. Melamed, N. *et al.* Neurodevelopmental disorders among term infants exposed to antenatal corticosteroids during pregnancy : a population-based study. 3–10 (2019). doi:10.1136/bmjopen-2019-031197
48. Räikkönen, K., Gissler, M. & Kajantie, E. Associations Between Maternal Antenatal Corticosteroid Treatment and Mental and Behavioral Disorders in Children Supplemental content. *Jama* **323**, 1924–1933 (2020).
49. Tsiarli, M. A. *et al.* Antenatal dexamethasone exposure differentially affects distinct cortical neural progenitor cells and triggers long-term changes in murine cerebral architecture and behavior. *Translational psychiatry* (2017). doi:10.1038/tp.2017.65
50. Mcewen, B. S. Glucocorticoids , depression , and mood disorders : structural remodeling in the brain. *Metabolism Clinical and Experimental* **54**, 20–23 (2005).

Data availability

Scripts and data for the MRa-PheWAS analyses are openly available via https://osf.io/4ud6q/ for full transparency. Data for the bulk RNA-seq are deposited as BioProject under accession code PRJNA865917.

Acknowledgments

LD acknowledges support by the Joachim Herz Foundation. We thank Mira Erhart, dr. Michael Czisch and dr. Benoit Boula for informative discussions on the brain structural measures. We thank Nathalie Gerstner and dr. Janine Knauer-Arloth for discussion on data analysis.

Conflict of interest

The authors declare no conflict of interest.

580 **Authors' contributions**

581 ACK conceived the idea, designed and carried out experiments, performed analyses, provided critical intellectual
582 input, generated and revised the paper draft; CC designed and performed omics experiments, provided critical
583 intellectual input and revised the paper draft; CK designed and performed electroporation experiments, provided
584 critical intellectual input and revised the paper draft; LD performed analysis and revised the paper draft; MHL
585 performed cell biology experiments and revised the paper draft; NK & DP performed the phenome wide mendelian
586 randomization analysis and revised the paper draft; SR performed analysis and revised the paper draft; VS, BW,
587 MK & SS performed experiments; MRH supported project organization and experimental procedures; ML designed
588 and performed CRISPR-Cas9 experiments, provided critical intellectual input and revised the paper draft; SC
589 provided critical intellectual input and revised the paper draft; EBB conceived the idea, obtained funding, supervised
590 the study, designed experiments and analysis pipelines, provided critical intellectual input and contributed to paper
591 draft writing and revisions.

592